

3
4 **Running title:** SLC44A1 promotes AML progression
5

6 **SLC44A1 promotes AML progression and chemoresistance by regulating the Notch signaling
7 pathway**

8
9 Shuyun Cao^{1,2,3}, Chengyun Pan^{1,3}, Xiuying Hu^{1,2,3}, Tianzhen Hu^{1,3,4}, Yanju Li^{1,3}, Qin Fang⁵, Jishi
10 Wang^{1,2,3,4,6,*}

11
12 ¹Department of Hematology, Affiliated Hospital of Guizhou Medical University, Guiyang, China;
13

14 ²School of Clinical Medicine, Guizhou Medical University, Guiyang, China; ³Province Institute of
15 Hematology, Guiyang, China; ⁴Guizhou Province Hematopoietic Stem Cell Transplantation Centre
16 and Key Laboratory of Hematological Disease Diagnostic and Treatment Centre, Guiyang, China;

17 ⁵Department of Pharmacy, Affiliated Hospital of Guizhou Medical University, Guiyang, China;

18 ⁶National Clinical Research Center for Hematologic Diseases, The First Affiliated Hospital of
Soochow University, Soochow, China

19
20 *Correspondence: wangjishi9696@126.com

21
22 **Received May 18, 2025 / Accepted December 22, 2025**

23
24 Despite advances in treatment, acute myeloid leukemia (AML) remains a formidable therapeutic
25 challenge, highlighting the urgent need for novel biomarkers and therapeutic targets. The choline
26 transporter SLC44A1 has been implicated in cancer progression; however, its role in AML remains
27 largely unexplored. Here, we investigated the clinical relevance and molecular mechanisms of
28 SLC44A1 in AML. Analysis of The Cancer Genome Atlas (TCGA) datasets revealed significant
29 upregulation of SLC44A1 in AML patients, correlating with poor patient prognosis. Functional
30 studies demonstrated that SLC44A1 knockdown markedly inhibited AML cell proliferation and
31 enhanced chemosensitivity to cytarabine and venetoclax. RNA sequencing and pathway analysis
32 identified the NOTCH signaling pathway as a key downstream target of SLC44A1, which was
33 further validated by western blot. Collectively, our findings establish SLC44A1 as a crucial
34 regulator of AML progression and chemoresistance, highlighting its dual potential as a prognostic
35 biomarker and a therapeutic target.

36
37 **Key words:** SLC44A1; acute myeloid leukemia; proliferation; chemoresistance; Notch signaling

38
39
40 Acute myeloid leukemia (AML) is a hematological malignancy derived from hematopoietic stem
41 cells and progenitor cells, and it represents the most prevalent type of leukemia in adults, with a
42 median age of onset of 68 years [1]. Over recent decades, the treatment paradigm for AML has
43 evolved from standard chemotherapy regimens, such as the "3+7" protocol, to novel targeted
44 therapies, including venetoclax, Sorafenib, among others [2]. Despite improvements in prognosis,
45 the survival rate for patients over 65 years old remains low, with a persistent risk of relapse and
46 refractory disease [3]. This underscores the urgent need for novel biomarkers to enhance diagnostic
47 accuracy, predict survival outcomes, and guide therapeutic strategies.

48 The solute carrier family 44 (SLC44) proteins, also known as choline transporter-like proteins, are

49 involved in choline metabolism and have been implicated in cancer progression [4]. Choline
50 accumulation in tumors is mediated by SLC44, increasing the cell membrane synthesis during
51 active cell proliferation in several cancer types [5-7]. Among them, SLC44A1 plays a crucial role in
52 choline transport across the plasma and mitochondrial membranes supporting synthesis pathways
53 essential for cell growth [8]. Notably, emerging evidence suggests that SLC44A1 is involved in
54 tongue squamous cell carcinoma, small cell lung carcinoma, pancreatic cancer cell proliferation,
55 migration, and metastasis [9-11]. However, its role in AML remains largely unexplored.

56 In this study, we investigated the expression levels of *SLC44A1* in AML and examined its
57 association with clinicopathological features and patient prognosis. Additionally, we conducted
58 cellular experiments to elucidate the underlying mechanisms by which SLC44A1 contributes to
59 AML progression and chemoresistance. Our study evaluates the potential of SLC44A1 as a
60 diagnostic marker and therapeutic target in AML.

61

62 Patients and methods

63 **Gene expression analysis.** The TIMER 2.0 [12] website (<https://compbio.cn/timer2/>) and The Gene
64 Expression Profiling Interactive Analysis (GEPIA) [13] platform (<http://gepia.cancer-pku.cn/>) was
65 employed to analyze the expression of the SLC44 family in pan-cancer compared to normal tissues.
66 The Gene Expression Omnibus (GEO) database [14] (<https://www.ncbi.nlm.nih.gov/geo/>) was used
67 for external validation. Data from GSE103424 dataset [15] was analyzed to evaluate differential
68 SLC44A1 expression patterns in relation to treatment response. Data obtained from The Cancer
69 Genome Atlas (TCGA) [16] (<https://tcga-data.nci.nih.gov/tcga/>) and the Genotype-Tissue
70 Expression (GTEx) [17] (<https://gtexportal.org/home>) databases were used to explore the
71 correlations between SLC44A1 expression levels, clinicopathological parameters, and prognosis.
72 Additionally, LinkedOmics [18] (<http://www.linkedomics.org/login.php>) was utilized to investigate
73 associations between SLC44A1 expression and molecular features. Based on GSE116256 [19]
74 dataset, SLC44A1 levels within single-cell data were displayed by “Nebulosa” R package.
75 Differential SLC44A1 expression in diverse cells was analyzed with “Libra” package. The
76 relationships of SLC44A expression with cancerous hematopoietic cells in certain differentiation
77 stages were provided by BloodSpot [20] (<https://www.fobinf.com/>).

78 **Patient samples and cell lines.** A total of 28 bone marrow specimens were collected from patients
79 with acute myeloid leukemia (AML) and healthy donors at the Affiliated Hospital of Guizhou
80 Medical University between 2022 and 2023 using simple random sampling. Clinical characteristics
81 of patients are summarized in Supplementary Table S1. Bone marrow mononuclear cells from AML
82 patients and healthy donors were isolated by Ficoll density gradient centrifugation. This study was

83 approved by the Institutional Research Ethics Committee, and written informed consent was
84 obtained from all participants.

85 The human AML cells (THP1 and MV4-11) were obtained from the ATCC (American Type Culture
86 Collection, USA) and authenticated before use. Cells were cultured in a medium supplemented with
87 10% certified heat-inactivated fetal bovine serum (FBS; SAFC Bioscience, Lenexa, KS) and
88 penicillin (Sigma Life Sciences, St. Louis, MO) and incubated under 37 °C with 5% CO₂.

89 **Immunofluorescence.** Fixed cells in 4% paraformaldehyde (4 °C, overnight), then washed with
90 PBS (×3). Permeabilization was performed with Triton X-100 (15 min), followed by PBS washes
91 (×3). After blocking with goat serum (1 h), cells were incubated with anti-SLC44A1 primary
92 antibody (1:200, 4 °C, 24 h) and washed (PBS, ×3). A CoraLite594-conjugated secondary antibody
93 (1:100, 1 h) was applied. Nuclei were counterstained with DAPI, and images were acquired using
94 an Olympus BX51 fluorescence microscope.

95 **Lentiviral transfection.** The SLC44A1-silencing RNA (shSLC44A1) was acquired from the
96 Genechem Co. Ltd. (Shanghai, China). Following specific instructions, we transfected the empty
97 vector and SLC44A1-shRNA into the THP-1 and MV4-11 cells. The shRNA sequence for
98 SLC44A1 was 5'-GAGCAGCTTCAGATAGCTGAA-3'. The sequence for the control shRNA was
99 5'-TTCTCCGAACGTGTCACGT-3'. Western blot was used to determine the transfection
100 efficiency. Lentivirus-infected cells were selected with puromycin at a final concentration of 3
101 µg/ml for THP-1 cells and 2 µg/ml for MV4-11 cells.

102 **Western blot.** A radioimmunoprecipitation (RIPA) lysis buffer that contained 1%
103 phenylmethylsulfonyl fluoride (PMSF) (Solarbio Science & Technology, Beijing, PRC) was added
104 to extract the total cellular proteins under 30 min of agitation. After this, extracts were collected
105 using 15 min of centrifugation at 12,000 × g and 4 °C to obtain the supernatants. Subsequently, a
106 bicinchoninic acid (BCA) kit (Solarbio, China) was used to detect the protein content. The 20 µg
107 proteins were later isolated by loading on 10% SDS-PAGE before being transferred onto
108 polyvinylidene difluoride (PVDF) membranes 120 V/250 mA. Subsequently, the membrane was
109 blocked by 5% nonfat milk for two hours. This was followed by another two hours of primary
110 antibody SLC44A1 (#14687-1-AP 1:1000); βactin (#K006153P 1:1000); NOTCH2 (#ERP26111-69
111 1:1000); APH1A (#YN6455 1:1000) incubation at ambient temperature or overnight incubation
112 under 4 °C. Moreover, the HRP-labeled Affinipure Goat Anti-Rabbit IgG secondary antibody
113 (H + L) was utilized. An electrochemiluminescence (ECL) kit (4 A Biotech, China) was used to
114 investigate the protein bands, and Image J was used for the quantification.

115 **Cell viability assay.** Cells were seeded (2 × 10³/well) onto 96-well plates for 1, 3, 5 days and
116 evaluated the cell viability using the Cell Counting Kit-8 (Target Molecule Corp, China). A

117 microplate ultra-micro spectrophotometer was used to evaluate the absorbance at 450 nm.

118 **Drug sensitivity assay.** For chemosensitivity evaluation, cells were plated at 1×10^4 cells/well in

119 96-well plates and exposed to gradient concentrations of Venetoclax (0, 2, 4, 8 nM for MV4-11; 0,

120 50, 150, 200 nM for THP1) and Cytarabine (0, 0.25, 0.5, 1 μ M for MV4-11 and THP1) for 24 h.

121 Following drug treatment, cell viability was quantified using the CCK-8 assay described above. The

122 proportion of apoptotic cells was determined using the Annexin V-APC/7-AAD Apoptosis Kit

123 (MultiSciences, China) according to the manufacturer's protocol. Cells were plated in 6-well plates

124 at a density of 1×10^5 cells/well and treated with drugs for 24 h, then analyzed on a FACSCalibur

125 instrument (BD Biosciences, San Jose, CA, USA).

126 **EdU incorporation assay.** In accordance with the manufacturer's instructions provided by the

127 producer, the cell-Light™ EdU Apollo567 In Vitro Kit (#C10310-1, Ribobio) was used for the EdU

128 incorporation assay.

129 **RNA-sequencing analysis.** Total cellular RNA was extracted using the TRIzol reagent kit

130 (Invitrogen, Carlsbad, CA, USA). RNA quality was evaluated with the Agilent 2100 Bioanalyzer

131 (Agilent Technologies, Santa Clara, CA, USA). Sequencing libraries were prepared using the

132 NEBNext Ultra RNA Library Prep Kit for Illumina (#E7770, New England Biolabs, Ipswich, MA,

133 USA). RNA sequencing was performed on the Illumina NovaSeq 6000 platform by Gene Denovo

134 Biotechnology Co (Guangzhou, China). Read quality was assessed using FastQC, and gene

135 expression levels were quantified with RSEM. Differentially expressed genes were identified based

136 on thresholds of $FDR < 0.05$ and $|\log_2 \text{fold change (FC)}| > 1.5$. The raw sequencing data have been

137 deposited in National Center for Biotechnology Information (NCBI) repository under the accession

138 number PRJNA1223631.

139 **Statistical analyses.** The Shapiro-Wilk test was used to check whether the continuous variables of

140 the different groups conformed to normal distributions. Non-normally distributed data were

141 explored using the Wilcoxon rank-sum test, or they were compared using the Mann-Whitney U test

142 or a student's t-test. A chi-square test or Fisher's exact test was utilized to compare the categorical

143 variables. A one-way analysis of variance (ANOVA) was employed to evaluate statistical

144 differences among multiple groups. R software (Version 4.3.1) was used for the analyses. $P < 0.05$

145 (two-tailed) was statistically significant.

146

147 **Results**

148 **SLC44A1 expression in pan-cancer.** We initiated our investigation with a comprehensive

149 pan-cancer analysis of the SLC44 protein family, which revealed that SLC44A1 exhibited the most

150 prominent upregulation across multiple malignancies (Supplementary Figures S1A, S1B). This

151 finding prompted us to focus specifically on SLC44A1 for subsequent analyses. Through systematic
152 evaluation using the TIMER 2.0 platform and GEPIA database, we compared SLC44A1 expression
153 profiles between tumor and adjacent normal tissues across 33 cancer types derived from TCGA.
154 Notably, among all SLC44 family members, SLC44A1 demonstrated significantly elevated
155 expression in 14 distinct cancer types, including bladder urothelial carcinoma (BLCA), breast
156 invasive carcinoma (BRCA), cervical squamous cell carcinoma (CESC), cholangiocarcinoma
157 (CHOL), colon adenocarcinoma (COAD), esophageal carcinoma (ESCA), head and neck squamous
158 cell carcinoma (HNSC), lung adenocarcinoma (LUAD), lung squamous cell carcinoma (LUSC),
159 stomach adenocarcinoma (STAD), diffuse large B-cell lymphoma (DLBC), acute myeloid leukemia
160 (AML), lower-grade glioma (LGG), and testicular germ cell tumors (TGCT). SLC44A1 protein
161 levels were elevated in solid tumors, including BRCA, CCRCC, UCEC, PAAD, and HNSC. In
162 contrast, its expression was reduced in COAD, OV, RCC, GBM, liver cancer (LC), and lung cancer
163 (Supplementary Figure S1C).

164 **Comprehensive evaluation of SLC44A1 expression in AML.** Comprehensive pan-cancer analysis
165 revealed that SLC44A1 exhibited the most pronounced overexpression in AML relative to normal
166 controls, prompting our subsequent evaluation of its clinical relevance in AML patients. The cohort
167 comprised 173 adult patients from the TCGA dataset, categorized into two groups according to the
168 median SLC44A1 expression level, with their clinicopathological characteristics summarized in
169 Table 1. Patients in the SLC44A1^{high} group exhibited elevated white blood cell (WBC) counts and
170 were more frequently associated with non-M3 subtypes, particularly M4 and M5, according to the
171 FAB classification. Also, SLC44A1^{high} group demonstrated a higher prevalence of NPM1 and FLT3
172 mutations and a poor cytogenetic risk profile (Table 1).

173 SLC44A1 expression was significantly elevated in patients with high tumor burden (WBC $\geq 10 \times$
174 $10^9 /l$) compared to those with lower WBC counts (Supplementary Figure S2A). Furthermore,
175 SLC44A1 was markedly upregulated in the poor cytogenetic risk group versus the favorable-risk
176 cohort (Supplementary Figure S2B). Notably, acute promyelocytic leukemia (APL) subtypes
177 displayed higher SLC44A1 expression than non-APL cases (Supplementary Figure S2C). Further
178 classification of patients based on the FAB subtypes revealed that SLC44A1 expression was highest
179 in the M5 subtype, followed by the M4 subtype (Supplementary Figure S2D). FLT3 and DNMT3A
180 mutations are known to be associated with poor prognosis in AML patients [21], data from the
181 LinkedOmics database indicated that SLC44A1 expression was markedly elevated in patients with
182 DNMT3A mutation (R882H) (Supplementary Figure S2E), FLT3 mutation (D835Y)
183 (Supplementary Figure S2F) and NPM1 mutation (W288F) (Supplementary Figure S2G) mutations
184 at the mRNA level. It should be noted that the prognostic significance of isolated NPM1 mutations

185 in favorable-risk AML patients remains limited. According to previous study [22], a comprehensive
186 prognostic evaluation must incorporate both *FLT3* mutational analysis and contemporary risk
187 stratification criteria. Furthermore, ROC analysis of the TCGA cohort revealed perfect diagnostic
188 discrimination (AUC=1.0) for *SLC44A1* in AML (Supplementary Figure S2H). To evaluate
189 differential *SLC44A1* expression patterns associated with treatment response, we analyzed the
190 GSE103424 dataset comprising 36 de novo acute myeloid leukemia (AML) samples, which were
191 stratified into complete remission (CR) and non-complete remission (non-CR) groups based on
192 their response to the standard "7+3" induction regimen (cytarabine plus daunorubicin). Notably, our
193 analysis revealed significantly higher *SLC44A1* expression levels in the non-CR group compared to
194 the CR group (Supplementary Figure S2I) in our center. These results indicate that *SLC44A1* could
195 be a promising candidate for further investigation as a diagnostic biomarker in AML.

196 **SLC44A1 correlates with poor prognosis in AML patients.** In the TCGA cohort, high *SLC44A1*
197 expression was associated with poorer overall survival (OS; $p < 0.001$, Supplementary Figure S3A)
198 and event-free survival (EFS; $p < 0.001$, Supplementary Figure S3B). Even within the
199 good/intermediate-risk groups, the *SLC44A1*^{high} group demonstrated significantly worse OS
200 ($p=0.00373$, Supplementary Figure S3C) and EFS ($p=0.0168$, Supplementary Figure S3D).

201 Using univariate analysis, (Table 2) age ≥ 60 years ($p < 0.001$), *FLT3* mutation ($p=0.039$), *DNMT3A*
202 mutation ($p=0.012$), *RUNX1* mutation ($p=0.047$), intermediate/poor risk level ($p < 0.001$), and high
203 *SLC44A1* expression ($p=0.011$) were associated with inferior OS. Consistently, WBC count $\geq 10 \times$
204 $10^9/l$ ($p=0.004$), *FLT3* mutation ($p=0.035$), intermediate/poor risk level ($p < 0.001$), and high
205 *SLC44A1* expression ($p=0.047$) were associated with inferior EFS (Table 2). However, multivariate
206 analysis revealed that age ≥ 60 was the only independent risk factor for both OS and EFS ($p <$
207 0.001).

208 Based on the multivariate Cox analysis, a predictive nomogram was constructed to estimate 1-, 3-,
209 and 5-year OS and EFS (Supplementary Figures S2G, S2H). The area under the curve (AUC) values
210 for the nomogram were 0.799, 0.823, and 0.878 for 1-, 3-, and 5-year OS, respectively
211 (Supplementary Figure S3E), and 0.773, 0.732, and 0.894 for 1-, 3-, and 5-year EFS, respectively
212 (Supplementary Figure S3F), demonstrating robust predictive specificity and sensitivity.

213 **Stage-specific expression pattern of *SLC44A1* in hematopoietic differentiation and validation**
214 **in single-cell data.** BloodSpot analysis revealed stage-specific *SLC44A1* expression patterns in
215 hematopoietic differentiation, showing predominant expression in promonocytes (Supplementary
216 Figure S4A). This observation was validated by the single-cell RNA sequencing data analysis
217 (Supplementary Figures S4B, S4C), consistent with our previous finding of *SLC44A1*
218 overexpression in FAB-M4/M5 AML subtypes.

219 **Knockdown of SLC44A1 decreased AML cell proliferation.** Immunofluorescence staining
220 confirmed the expression of SLC44A1 in M4/M5-representative cell lines (THP-1 and MV4-11)
221 and primary AML samples, revealing its dual nuclear and cytoplasmic localization (Figure 1A).
222 Consistent with this, an initial analysis of our institutional cohort demonstrated that SLC44A1
223 expression was significantly elevated in AML patients compared to healthy controls, at both the
224 protein (Figures 1B, 1C) and mRNA levels (Figure 1D). To further investigate the functional role of
225 SLC44A1 in AML, we knock down SLC44A1 by lentivirus infection (Figure 1E). Cell Counting
226 Kit-8 (CCK-8) and the 5-Ethynyl-2'-deoxyuridine (EdU) incorporation assays were performed to
227 evaluate the effect of SLC44A1 on AML cell proliferation. CCK-8 assay was performed to evaluate
228 the effect of SLC44A1 on AML cell viability (Figures 1F, 1G). In parallel, the EdU incorporation
229 assays were utilized to assess the effect of SLC44A1 on AML cell proliferation (Figures 1H-1K).
230 The results demonstrated that the knockdown of SLC44A1 significantly suppressed the
231 proliferation of MV4-11 and THP1 cells. These findings suggested that SLC44A1 plays a critical
232 role in promoting AML cell proliferation.

233 **SLC44A1 regulated the therapeutic efficacy of AML.** Bioinformatics analysis revealed elevated
234 SLC44A1 expression in AML patients who failed to achieve CR following conventional
235 chemotherapy regimens, suggesting a potential association between SLC44A1 and chemoresistance.
236 To further investigate this association, we systematically evaluated the role of SLC44A1 in
237 modulating drug sensitivity using two clinically relevant agents: cytarabine (a conventional
238 chemotherapeutic drug) and venetoclax (a novel targeted therapy and one of the most frequently
239 prescribed agents in AML treatment). Functional assays demonstrated that SLC44A1
240 downregulation significantly enhanced the sensitivity of both THP1 and MV4-11 cells to these
241 therapeutic agents (Figures 2A-2D). Consistently, apoptosis assays further confirmed that SLC44A1
242 downregulation enhanced the sensitivity of THP-1 and MV4-11 cells to both cytarabine and
243 venetoclax, further validating its role in therapeutic resistance (Figures 2E, 2F). These findings
244 indicated that SLC44A1 plays a critical role in modulating therapeutic resistance in AML.

245 **SLC44A1 affects AML progression through the NOTCH signaling pathway.** To explore the
246 underlying mechanisms by which SLC44A1 influences AML malignancy. We analyzed the gene
247 expression profile of SLC44A1 knockdown cells using RNA-seq. Based on the RNA-sequencing
248 data, we found that 573 genes were upregulated and 1251 genes were downregulated in SLC44A1
249 MV4-11 cell lines (Figure 3A). The list of the top 100 significantly upregulated and downregulated
250 genes has been provided in Supplementary data 1. Gene Ontology (GO) enrichment analysis
251 demonstrated that SLC44A1 is significantly enriched in cellular response to chemical stimulus
252 (Figure 3B), providing a potential mechanistic explanation for its role in chemoresistance.

253 Furthermore, SLC44A1 was found to be involved in critical cellular signaling transduction
254 processes, particularly in cell surface receptor signaling pathway and regulation of signaling (Figure
255 3B). These findings prompted us to perform KEGG pathway enrichment analysis, which identified
256 the NOTCH signaling pathway as a critical mediator of SLC44A1-driven AML pathogenesis.
257 Subsequent experimental validation revealed that this pathway is associated with the anti-leukemic
258 effects of SLC44A1 knockdown (Figure 3C). Previous studies have shown that activation of the
259 NOTCH pathway induces tumorigenesis and progression in AML [23]. Subsequently, we compared
260 the expression levels of NOTCH pathway-related proteins between SLC44A1-knockdown AML
261 cells and the control, as NOTCH2 and APH1A were the most significantly affected targets
262 identified in the RNA-seq analysis. Both NOTCH2 and APH1A were significantly downregulated
263 in SLC44A1 knockdown cells (Figures 3D-3F). These results suggested that SLC44A1 promotes
264 AML cell proliferation and drug resistance by regulating the NOTCH signaling pathway,
265 highlighting a potential mechanism underlying SLC44A1 - mediated AML malignancy.
266

267 **Discussion**

268 Despite the development of novel therapies over the past decades, the prognosis for adult AML
269 patients remains poor, especially for those over 65 years old, with a 5-year overall survival rate of
270 only 30% [24]. Thus, a deeper understanding of the molecular mechanisms underlying AML
271 pathogenesis and the identification of novel therapeutic targets is essential for advancing targeted
272 therapies. This study identified SLC44A1 is highly expressed in adult AML patients compared with
273 healthy donors and is associated with poor clinicopathological features. Furthermore, SLC44A1
274 exhibited excellent diagnostic value and was linked to an unfavorable prognosis. Based on the
275 functional analysis for SLC44A1, we found that SLC44A1 knockdown inhibited the proliferation of
276 AML cells and enhanced chemosensitivity, highlighting its potential as a therapeutic target in AML.
277 While SLC44A2 has been documented as a prognostic marker in acute myeloid leukemia (AML)
278 based on the UALCAN [25] database (<https://ualcan.path.uab.edu/>), the clinical relevance of
279 SLC44A1 in AML remains largely undefined. To address this gap, we systematically evaluated the
280 relationship between SLC44A1 expression and disease outcomes in AML. Our results reveal that
281 high SLC44A1 expression is significantly associated with adverse risk stratification, co- occurrence
282 of poor-prognosis genetic alterations, and shorter overall survival (OS) and event- free survival
283 (EFS). Collectively, these data support the potential utility of SLC44A1 as a prognostic biomarker
284 in AML. Consistently, in breast cancer (BC), SLC44A1 was significantly linked to OS,
285 progression-free survival (PFS), and an increased risk of bone metastasis [26]. Additionally, in head
286 and neck cancer (HNC), SLC44A1 showed higher expression in high-grade (III/IV) tumors

287 compared to low-grade (I/II) tumors [27]. Expression of SLC44A1 was significantly correlated with
288 disease-specific survival (DSS) and PFS. A large-scale analysis involving approximately 2,000
289 multiple myeloma patients confirmed its correlation with poor prognosis [28], suggesting that
290 SLC44A1 may serve as a potential biomarker for disease progression and unfavorable clinical
291 outcomes in MM patients. To further establish the prognostic value of SLC44A1 in AML, studies
292 involving large clinical cohorts are required.

293 In this study, we investigated the role of SLC44A1 in AML cell proliferation and chemosensitivity.
294 Choline is an essential nutrient involved in multiple biological processes, including the synthesis of
295 the membrane lipid phosphatidylcholine (PtdCho) [29]. Dysregulated choline metabolism is a
296 well-established hallmark of proliferation drug resistance and has been implicated in various cancer
297 types [30, 31]. Notably, as a choline transporter, SLC44A1 has been implicated in the increased
298 synthesis of the membrane lipid phosphatidylcholine (PtdCho), which is associated with drug
299 resistance in both rectal and pancreatic cancers [32, 33]. Therefore, SLC44A1-mediated AML
300 malignant progression may be regulated by choline metabolism. Resistance to cytarabine and
301 venetoclax in acute myeloid leukemia (AML) involves complex and multifactorial mechanisms.
302 Cytarabine resistance may arise not only from impaired cellular uptake due to reduced expression of
303 nucleoside transporters such as hENT1 and hCNT1, altered mitochondrial metabolism characterized
304 by decreased oxidative phosphorylation, or enhanced DNA repair capacity, but also from
305 dysregulated signaling pathways and adaptations within the tumor microenvironment [34-37]. In
306 contrast, resistance to venetoclax is frequently driven by the upregulation of anti-apoptotic proteins
307 (e.g., MCL-1, BCL-XL), mutations in BAX, or activation of oncogenic pathways such as N/KRAS,
308 FLT3-ITD, and TP53 [38-40]. To our knowledge, this is the first study to demonstrate that
309 downregulation of SLC44A1 enhances the chemosensitivity of AML cells, addressing a critical gap
310 in the current literature. Our findings suggest that SLC44A1 may represent one of the contributing
311 factors to such resistance; however, its precise mechanistic role and significance within the broader
312 resistance network warrant further elucidation through additional *in vitro* and *in vivo* studies.
313 The observed suppression of AML cell proliferation and enhanced chemosensitivity following
314 SLC44A1 knockdown merit mechanistic investigation. Our data suggest that this phenotype may be
315 mediated through inhibition of the NOTCH signaling pathway, as evidenced by the concomitant
316 downregulation of key NOTCH-related proteins. Furthermore, SLC44A1 knockdown in AML cells
317 significantly reduced the expression of NOTCH pathway components (NOTCH2 and APH1A),
318 while NOTCH agonist treatment partially reversed the phenotypic effects of SLC44A1 knockdown.
319 NOTCH is an important signaling pathway in cancer, playing a vital role in tumor initiation and
320 progression [41, 42]. Importantly, activation of the NOTCH signaling pathway triggered abnormal

321 leukemic stem cell activation, promoting tumor proliferation and drug resistance [43-45], while
322 downregulation of NOTCH2 has been shown to inhibit AML proliferation [46]. Furthermore,
323 NOTCH activation stimulates bone marrow mesenchymal stromal cells to facilitate AML
324 progression and confer resistance to chemotherapy [47]. As a component of the plasma membrane,
325 the Notch receptor plays a crucial role in activating the NOTCH signaling pathway [48].
326 Intriguingly, SLC44A1, which our GO analysis identified as being enriched in cell surface receptor
327 signaling pathways, has been implicated in plasma membrane biosynthesis [49]. These findings
328 collectively suggest that SLC44A1 may regulate AML proliferation and drug resistance through
329 modulation of NOTCH receptor or membrane integration, thereby influencing NOTCH signaling
330 activation.

331 In conclusion, this study identifies SLC44A1 as a key driver of AML pathogenesis and highlights
332 its potential as both a prognostic biomarker and a therapeutic target. Future research should focus
333 on deciphering the downstream signaling pathways regulated by SLC44A1 and its interactions with
334 other oncogenic drivers in AML. Additionally, investigating the therapeutic efficacy of SLC44A1
335 inhibitors in preclinical AML models will be essential for advancing targeted treatment strategies.
336

337 **Acknowledgements:** The TCGA, GEO (Accession: GSE103424, GSE116256), and GTEx data used
338 for bioinformatics analysis are accessible through their respective portals. The datasets generated
339 during the current study are available in the National Center for Biotechnology Information (NCBI)
340 repository, [BioProject ID PRJNA1223631].

341 This work was supported by the National Natural Science Foundation of China (82170168,
342 82370168, 82260728); the Guizhou Provincial Basic Research Program (Natural Science) (Qian Ke
343 He-ZK [2023] No.382); the Foundation the Translational Research Grant of NCRCH
344 (2021WWB01); and the Cultivation Project of National Natural Science Foundation of Guizhou
345 Medical University (Academic new seedlings) (20NSP027, Gfynsf-2021-3).
346

347 **Supplementary data are available in the online version of the paper.**
348
349

350 **References**

- 351 [1] SHIMONY S, STAHL M, STONE RM. Acute myeloid leukemia: 2023 update on diagnosis,
352 risk-stratification, and management. *Am J Hematol* 2023; 98: 502-526.
353 <https://doi.org/10.1002/ajh.26822>
- 354 [2] FORSBERG M, KONOPLEVA M. Aml treatment: conventional chemotherapy and
355 emerging novel agents. *Trends Pharmacol Sci* 2024; 45: 430-448.
356 <https://doi.org/10.1016/j.tips.2024.03.005>

357 [3] BHANSALI RS, PRATZ KW, LAI C. Recent advances in targeted therapies in acute
358 myeloid leukemia. *J Hematol Oncol* 2023; 16: 29.
359 <https://doi.org/10.1186/s13045-023-01424-6>

360 [4] SONG T, ZHAO S, LUO S, CHEN C, LIU X et al. Slc44a2 regulates vascular smooth
361 muscle cell phenotypic switching and aortic aneurysm. *J Clin Invest* 2024; 134: e173690.
362 <https://doi.org/10.1172/JCI173690>

363 [5] HIRAI K, WATANABE S, NISHIJIMA N, SHIBATA K, HASE A et al. Molecular and
364 functional analysis of choline transporters and antitumor effects of choline transporter-like
365 protein 1 inhibitors in human pancreatic cancer cells. *Int J Mol Sci* 2020; 21: 5190.
366 <https://doi.org/10.3390/ijms21155190>

367 [6] GLUNDE K, BHUJWALLA ZM, RONEN SM. Choline metabolism in malignant
368 transformation. *Nat Rev Cancer* 2011; 11: 835-848. <https://doi.org/10.1038/nrc3162>

369 [7] HE J, WANG A, ZHAO Q, ZOU Y, ZHANG Z et al. Rnai screens identify hes4 as a
370 regulator of redox balance supporting pyrimidine synthesis and tumor growth. *Nat Struct
371 Mol Biol* 2024 2024; 31: 1413-1425. <https://doi.org/10.1038/s41594-024-01309-3>

372 [8] FAGERBERG CR, TAYLOR A, DISTELMAIER F, SCHRODER HD, KIBAEK M et al.
373 Choline transporter-like 1 deficiency causes a new type of childhood-onset
374 neurodegeneration. *Brain* 2020; 143: 94-111. <https://doi.org/10.1093/brain/awz376>

375 [9] SHIBATA K, NISHIJIMA N, HIRAI K, WATANABE S, YAMANAKA T et al. A novel
376 plant-derived choline transporter-like protein 1 inhibitor, amb544925, induces apoptotic cell
377 death via the ceramide/survivin pathway in tongue squamous cell carcinoma. *Cancers
378 (Basel)* 2022; 14: 329. <https://doi.org/10.3390/cancers14020329>

379 [10] INAZU M, YAMADA T, KUBOTA N, YAMANAKA T. Functional expression of choline
380 transporter-like protein 1 (ctl1) in small cell lung carcinoma cells: a target molecule for lung
381 cancer therapy. *Pharmacol Res* 2013; 76: 119-131.
382 <https://doi.org/10.1016/j.phrs.2013.07.011>

383 [11] INAZU M, HIRAI K, WATANABE S, NISHIJIMA N, SHIBATA K et al. 25p development
384 of new therapeutic drugs for pancreatic cancer targeting choline transporter-like protein 1
385 (ctl1/slcs44a1). *Ann Oncol* 2020; 31: S8-09. <https://doi.org/10.1016/j.annonc.2020.01.044>

386 [12] LI T, FU J, ZENG Z, COHEN D, LI J et al. Timer2.0 for analysis of tumor-infiltrating
387 immune cells. *Nucleic Acids Res* 2020; W509-514. <https://doi.org/10.1093/nar/gkaa407>

388 [13] TANG Z, LI C, KANG B, GAO G, LI C et al. Gepia: a web server for cancer and normal
389 gene expression profiling and interactive analyses. *Nucleic Acids Res* 2017; 45: W98-102.
390 <https://doi.org/10.1093/nar/gkx247>

391 [14] EDGAR R, DOMRACHEV M, LASH AE. Gene expression omnibus: ncbi gene expression
392 and hybridization array data repository. *Nucleic Acids Res* 2002; 30: 207-210.
393 <https://doi.org/10.1093/nar/30.1.207>

394 [15] CHIU Y, HSIAO T, TSAI J, WANG L, HO T et al. Integrating resistance functions to predict
395 response to induction chemotherapy in de novo acute myeloid leukemia. *Eur J Haematol*
396 2019; 103: 417-425. <https://doi.org/10.1111/ejh.13301>

397 [16] CANCER GENOME ATLAS RESEARCH NETWORK, WEINSTEIN JN, COLLISON
398 EA, MILLS GB, SHAW KRM et al. The cancer genome atlas pan-cancer analysis project.
399 *Nat Genet* 2013; 45: 1113-1120. <https://doi.org/10.1038/ng.2764>

400 [17] GTEx CONSORTIUM. Human genomics. The genotype-tissue expression (gtex) pilot
401 analysis: multitissue gene regulation in humans. *Science (New York, N.Y.)*; 348: 648-60.
402 <https://doi.org/10.1126/science.1262110>

403 [18] VASAIKAR SV, STRAUB P, WANG J, ZHANG B. Linkedomics: analyzing multi-omics
404 data within and across 32 cancer types. *Nucleic Acids Res* 2018; 46: D956-963.
405 <https://doi.org/10.1093/nar/gkx1090>

406 [19] VAN GALEN P, HOVESTADT V, WADSWORTH II MH, HUGHES TK, GRIFFIN GK et
407 al. Single-cell rna-seq reveals aml hierarchies relevant to disease progression and immunity.
408 Cell 2019; 176: 1265-1281. <https://doi.org/10.1016/j.cell.2019.01.031>

409 [20] GÍSLASON MH, DEMIRCAN GS, PRACHAR M, FURTWÄNGLER B, SCHWALLER J
410 et al. Bloodspot 3.0: a database of gene and protein expression data in normal and malignant
411 haematopoiesis. Nucleic Acids Res 2024; 52: D1138-1142.
412 <https://doi.org/10.1093/nar/gkad993>

413 [21] MROZEK K, KOHLSCHMIDT J, BLACHLY JS, NICOLET D, CARROLL AJ et al.
414 Outcome prediction by the 2022 european leukemianet genetic-risk classification for adults
415 with acute myeloid leukemia: an alliance study. Leukemia 2023; 37: 788-798.
416 <https://doi.org/10.1038/s41375-023-01846-8>

417 [22] FALINI B, DILLON R. Criteria for diagnosis and molecular monitoring of npm1-mutated
418 aml. Blood Cancer Discov 2024; 5: 8-20. <https://doi.org/10.1158/2643-3230.BCD-23-0144>

419 [23] RODRIGUES ACBD, COSTA RGA, SILVA SLR, DIAS IRSB, DIAS RB et al. Cell
420 signaling pathways as molecular targets to eliminate aml stem cells. Crit Rev Oncol Hematol
421 2021; 160: 103277. <https://doi.org/10.1016/j.critrevonc.2021.103277>

422 [24] LACHOWIEZ CA, LOGHAVI S, FURUDATE K, MONTALBAN-BRAVO G, MAITI A et
423 al. Impact of splicing mutations in acute myeloid leukemia treated with hypomethylating
424 agents combined with venetoclax. Blood Adv 2021; 5: 2173-2183.
425 <https://doi.org/10.1182/bloodadvances.2020004173>

426 [25] CHANDRASHEKAR DS, KARTHIKEYAN SK, KORLA PK, PATEL H, SHOVON AR et
427 al. Ualcan: an update to the integrated cancer data analysis platform. Neoplasia (New York,
428 N.Y.). 2022; 25: 18-27. <https://doi.org/10.1016/j.neo.2022.01.001>

429 [26] FAN TD, BEI DK, LI SW. Nomogram models based on the gene expression in prediction of
430 breast cancer bone metastasis. J Healthc Eng 2022; 2022: 8431946.
431 <https://doi.org/10.1155/2022/8431946>

432 [27] MA W, CAO Q, SHE W. Identification and clinical validation of gene signatures with grade
433 and survival in head and neck carcinomas. Braz J Med Biol Res 2021; 54: e11069.
434 <https://doi.org/10.1590/1414-431X2020e11069>

435 [28] GAROFANO F, CORSALE AM, SHEKARKAR AZGOMI M, DI SIMONE M, SPECIALE
436 M et al. Unveiling novel therapeutic targets for car therapy in multiple myeloma through
437 single-cell rna sequencing. Blood 2023; 142: 6605.
438 <https://doi.org/10.1182/blood-2023-188474>

439 [29] MA Q, JIANG H, MA L, ZHAO G, XU Q et al. The moonlighting function of glycolytic
440 enzyme enolase-1 promotes choline phospholipid metabolism and tumor cell proliferation.
441 Proc Natl Acad Sci U S A 2023; 120: e2085532176.
442 <https://doi.org/10.1073/pnas.2209435120>

443 [30] WEN S, HE Y, WANG L, ZHANG J, QUAN C et al. Aberrant activation of super enhancer
444 and choline metabolism drive antiandrogen therapy resistance in prostate cancer. Oncogene
445 2020; 39: 6556-6571. <https://doi.org/10.1038/s41388-020-01456-z>

446 [31] RIZZO A, SATTA A, GARRONE G, CAVALLERI A, NAPOLI A et al. Choline kinase alpha
447 impairment overcomes trail resistance in ovarian cancer cells. J Exp Clin Cancer Res 2021
448 2021; 40: 5. <https://doi.org/10.1186/s13046-020-01794-6>

449 [32] ANDREJEVA G, GOWAN S, LIN G, WONG TFA, SHAMSAEI E, et al. De novo
450 phosphatidylcholine synthesis is required for autophagosome membrane formation and
451 maintenance during autophagy. Autophagy 2020; 16: 1044-1060.
452 <https://doi.org/10.1080/15548627.2019.1659608>

453 [33] SAITO RF, ANDRADE L, BUSTOS SO, CHAMMAS R. Phosphatidylcholine-derived lipid
454 mediators: the crosstalk between cancer cells and immune cells. Front Immunol 2022; 13:
455 768606. <https://doi.org/10.3389/fimmu.2022.768606>

456 [34] JARAMILLO AC, HUBECK I, BROEKHUIZEN R, PASTOR-ANGLADA M, KASPERS
457 GJL et al. Expression of the nucleoside transporters hnt1 (slc29) and hcnt1 (slc28) in
458 pediatric acute myeloid leukemia. *Nucleosides Nucleotides Nucleic Acids* 2020; 39:
459 1379-1388. <https://doi.org/10.1080/15257770.2020.1746803>

460 [35] YEON CHAE S, JANG S, KIM J, HWANG S, MALANI D et al. Mechanisms of
461 chemotherapy failure in refractory/relapsed acute myeloid leukemia: the role of cytarabine
462 resistance and mitochondrial metabolism. *Cell Death Dis* 2025; 16: 331.
463 <https://doi.org/10.1038/s41419-025-07653-6>

464 [36] WU J, LI X, LIU Y, CHEN G, LI R et al. Mmp14 from bm-mscs facilitates progression and
465 ara-c resistance in acute myeloid leukemia via the jak/stat pathway. *Exp Hematol Oncol*
466 2025; 14: 43. <https://doi.org/10.1186/s40164-025-00635-6>

467 [37] SHIVHARE K, SATIJA NK. Acute myeloid leukemia-osteoblast interaction mediated
468 autophagy induction protects against cytarabine induced apoptosis. *Cell Biochem Funct*
469 2025; 43: e70055. <https://doi.org/10.1002/cbf.70055>

470 [38] WANG Z, LAI R, WANG X, CHEN X, ZHOU Y et al. Targeted penetrating motif
471 engineering of bh3 mimetic: harnessing non-canonical amino acids for coinhibition of mcl-1
472 and bcl-xl in acute myeloid leukemia. *Adv Sci (Weinh)* 2025; 12: e2503682.
473 <https://doi.org/10.1002/advs.202503682>

474 [39] MOUJALLED DM, BROWN FC, CHUA CC, DENGLER MA, POMILIO G et al. Acquired
475 mutations in bax confer resistance to bh3-mimetic therapy in acute myeloid leukemia. *Blood*
476 2023; 141: 634-644. <https://doi.org/10.1182/blood.2022016090>

477 [40] LACHOWIEZ CA, HEIBLIG M, ASPAS REQUENA G, TAVERNIER-TARDY E, DAI F et
478 al. Genetic and phenotypic correlates of clinical outcomes with venetoclax in acute myeloid
479 leukemia: the gen-phen-ven study. *Blood Cancer Discov* 2025; 6: 437-449.
480 <https://doi.org/10.1158/2643-3230.BCD-24-0256>

481 [41] ZHOU B, LIN W, LONG Y, YANG Y, ZHANG H et al. Notch signaling pathway:
482 architecture, disease, and therapeutics. *Signal Transduct Target Ther* 2022; 7: 95.
483 <https://doi.org/10.1038/s41392-022-00934-y>

484 [42] SHI Q, XUE C, ZENG Y, YUAN X, CHU Q et al. Notch signaling pathway in cancer:
485 from mechanistic insights to targeted therapies. *Signal Transduct Target Ther* 2024; 9: 128.
486 <https://doi.org/10.1038/s41392-024-01828-x>

487 [43] TOMASONI C, ARSUFFI C, DONSANTE S, CORSI A, RIMINUCCI M et al. Aml alters
488 bone marrow stromal cell osteogenic commitment via notch signaling. *Front Immunol* 2023;
489 14: 1320497. <https://doi.org/10.3389/fimmu.2023.1320497>

490 [44] NAEF P, RADPOUR R, JAEGER-RUCKSTUHL CA, BODMER N, BAERLOCHER GM
491 et al. Il-33-st2 signaling promotes stemness in subtypes of myeloid leukemia cells through
492 the wnt and notch pathways. *Sci Signal* 2023; 16: eadd7705.
493 <https://doi.org/10.1126/scisignal.add7705>

494 [45] LAINEZ-GONZALEZ D, SERRANO-LOPEZ J, ALONSO-DOMINGUEZ JM.
495 Understanding the notch signaling pathway in acute myeloid leukemia stem cells: from
496 hematopoiesis to neoplasia. *Cancers (Basel)* 2022; 14: 1459.
497 <https://doi.org/10.3390/cancers14061459>

498 [46] MA X, ZHANG W, ZHAO M, LI S, JIN W et al. Oncogenic role of lncrna crnde in acute
499 promyelocytic leukemia and npml-mutant acute myeloid leukemia. *Cell Death Discov*
500 2020; 6: 121. <https://doi.org/10.1038/s41420-020-00359-y>

501 [47] TAKAM KP, BASSI G, CASSARO A, MIDOLO M, DI TRAPANI M et al. Notch signalling
502 drives bone marrow stromal cell-mediated chemoresistance in acute myeloid leukemia.
503 *Oncotarget* 2016; 7: 21713-21727. <https://doi.org/10.18632/oncotarget.7964>

504 [48] MEDINA E, PEREZ DH, ANTFLK D, LUCA VC. New tricks for an old pathway: emerging
505 notch-based biotechnologies and therapeutics. *Trends Pharmacol Sci* 2023; 44: 934-948.
506 <https://doi.org/10.1016/j.tips.2023.09.011>

507 [49] TAYLOR A, GRAPENTINE S, ICHHPUNIANI J, BAKOVIC M. Choline transporter-like
508 proteins 1 and 2 are newly identified plasma membrane and mitochondrial ethanolamine
509 transporters. *J Biol Chem* 2021; 296: 100604. <https://doi.org/10.1016/j.jbc.2021.100604>

510
511 **Figure Legends**

512

513 **Figure 1.** Effects of SLC44A1 knockdown on the proliferation of AML cells. A)
514 Immuno fluorescence staining confirmed the subcellular localization of SLC44A1 in AML cell lines
515 (THP-1 and MV4-11) and primary AML samples. B) The expression of SLC44A1 was validated in
516 the AML patients and normal subjects by western blot, and the relative protein level of SLC44A1
517 was analyzed by Image J (C). D) The mRNA level of SLC44A1 in the AML patients and healthy
518 donors was detected by qRT-PCR. E) Knockdown efficiency of SLC44A1 by shSLC44A1 in
519 MV4-11 and THP1 cells. The CCK8 analyses revealed that the SLC44A1 knockdown caused a
520 significant reduction in MV4-11 (F) and THP1 (G) cell proliferation (The initial number of cultured
521 cells was 2×10^3 /well). H-K) The EdU incorporation test suggested that the inhibition of SLC44A1
522 weakened MV4-11 (H, I) and THP1 (J, K) cell growth (scale bar=200 μ m). All experiments were
523 repeated three times independently. Data were analyzed using two tailed Student's t-test (F, G, I, K).

524 *p < 0.05; **p < 0.01; ***p < 0.001

525

526 **Figure 2.** SLC44A1 knockdown enhanced chemo-sensitivity to AML cells. A, B) The proliferation
527 of SLC44A1-knockdown THP-1 (A) and MV4-11(B) cell lines was assessed following the
528 treatment of cytarabine. C, D) The proliferation of SLC44A1 -knockdown THP-1 (C) and MV4-11
529 (D) cell lines was assessed following treatment of venetoclax. E, F) Cell apoptosis was detected by
530 7-ADD/annexin V staining after 24 h of treatment with cytarabine (0.1 μ M for MV4-11, 0.2 μ M for
531 THP1) and venetoclax (2 nM for MV4-11, 50 nM for THP1). All experiments were repeated three
532 times independently. Data were analyzed using two tailed Student's t-test (A-F). *p < 0.05; **p <
533 0.01; ***p < 0.001

534

535 **Figure 3.** Transcriptomic Profiling and Pathway Analysis in MV4-11 Cells after SLC44A1
536 Knockdown. A) The illustration of the Volcano plot showed the changing of the gene expression
537 profile in SLC44A1 knockdown AML cells. B) Gene Ontology (GO) enrichment analysis of
538 slc44a1 targets. C) Kyoto Encyclopedia of Genes and Genomes (KEGG) analysis of identified
539 targets. D) The protein expression level of the NOTCH signaling pathway was detected by western
540 blot. All experiments were repeated three times independently. Data were analyzed using two
541 tailed-Student's t-test (E, F). *p < 0.05; **p < 0.01

542

Table 1. Clinicopathological features of the AML patients in the TCGA cohort.

Characteristics	Overall (N=173)	SLC44A1low (N=86)	SLC44A1high (N=87)	p-value
Sex (%)				0.197
Male	93 (53.8%)	42 (48.8%)	51 (58.6%)	
Female	80 (46.2%)	44 (51.2%)	36 (41.4%)	
Age (median [IQR])	58 [46-68]	59 [41-67]	58 [44-67]	0.787
WBC count ($\times 10^9/l$) (median [IQR])	18.5 [3.25-58.5]	10 [2-42.5]	30 [8-73]	0.001
BM blasts (%) (median [IQR])	48 [16-48]	53 [18-80]	47 [11-66]	0.201
PB blasts (%) (median [IQR])	71.5 [51-85.75]	69 [48-85]	72 [52-86]	0.525
FAB classifications (%)				0.002
M0	16 (9.2%)	12 (14.1%)	4 (4.7%)	
M1	42 (24.3%)	21 (24.7%)	21 (24.4%)	
M2	39 (22.5%)	20 (23.5%)	19 (22.1%)	
M3	16 (9.2%)	12 (14.1%)	4 (4.7%)	
M4	35 (20.2%)	14 (16.5%)	21 (24.4%)	
M5	18 (10.4%)	2 (2.4%)	16 (18.6%)	
M6	2 (1.2%)	2 (2.4%)	0 (0.00%)	
M7	3 (1.7%)	2 (2.4%)	1 (1.2%)	
FLT3 mutation (%)				0.032
Wild	124 (71.7%)	68 (79.1%)	56 (64.4%)	
Mutated	49 (28.3%)	18 (20.9%)	31 (35.6%)	
DNMT3A mutation (%)				
Wild	130 (75.1%)	70 (81.4%)	60 (69.0%)	0.059
Mutated	43 (24.9%)	16 (18.6%)	27 (31.0%)	
RUNX1 mutation (%)				0.583
Wild	157 (90.8%)	77 (89.5%)	80 (92.0%)	
Mutated	16 (9.2%)	9 (10.5%)	7 (8.0%)	
NPM1 mutation (%)				0.008
Wild	125 (72.3%)	70 (81.4%)	55 (63.2%)	
Mutated	48 (27.7%)	16 (18.6%)	32 (36.8%)	
IDH1 mutation (%)				0.583
Wild	157 (90.8%)	77 (89.5%)	80 (92.0%)	
Mutated	16 (9.2%)	9 (10.5%)	7 (8.0%)	
RAS mutation (%)				0.234
Wild	154 (89.0%)	79 (91.9%)	75 (86.2%)	
Mutated	19 (11.0%)	7 (8.1%)	12 (13.8%)	
Risk level (%)				
Good	32 (18.7%)	26 (30.6%)	6 (7.0%)	< 0.001
Intermediate	103 (60.2%)	38 (44.7%)	65 (75.6%)	
Poor	36 (21.1%)	21 (24.7%)	15 (17.4%)	

Table 2. Univariate analysis for OS and EFS.

Characteristics	Overall survival (OS)			Event-free survival (EFS)		
	HR	95%CI	p-value	HR	95%CI	p-value
Age (≥ 60 vs. < 60)	3.221	2.146-4.832	< 0.001	1.834	1.729-3.647	< 0.001
Sex (female vs. male)	1.008	0.676-1.503	0.97	0.912	0.674-1.422	0.912
WBC count (≥ 15 vs. < 15 × 10 ⁹ /l)	1.434	0.959-2.145	0.079	1.745	1.194-2.55	0.004
BM blasts (≥ 70% vs. < 70%)	1.187	0.795-1.772	0.403	1.14	0.785-1.653	0.492
PB blasts (≥ 30% vs. < 30%)	1.135	0.755-1.707	0.542	1.448	0.984-2.131	0.06
FLT3 (mutated vs. wild)	1.574	1.024-2.422	0.039	1.537	1.031-2.292	0.035
NPM1 (mutated vs. wild)	1.142	0.728-1.79	0.564	1.106	0.728-1.628	0.636
DNMT3A (mutated vs. wild)	1.775	1.133-2.781	0.012	1.469	0.962-2.242	0.075
IDH1 (mutated vs. wild)	0.785	0.38-1.619	0.511	0.827	0.431-1.584	0.566
RUNX1 (mutated vs. wild)	1.464	1.005-2.133	0.047	1.427	0.782-2.605	0.247
NRAS (mutated vs. wild)	0.526	0.166-1.665	0.275	0.918	0.374-2.254	0.853
KRAS (mutated vs. wild)	1.745	0.763-3.991	0.187	1.979	0.919-4.264	0.081
Risk (Intermediate/Poor vs. good)	1.745	1.834-6.884	< 0.001	2.88	1.638-5.063	< 0.001
SLC44A1 (high vs. low)	1.7	1.131-2.554	0.011	1.834	1.834-2.133	0.047

Accepted manuscript

Fig. 1 [Download full resolution image](#)

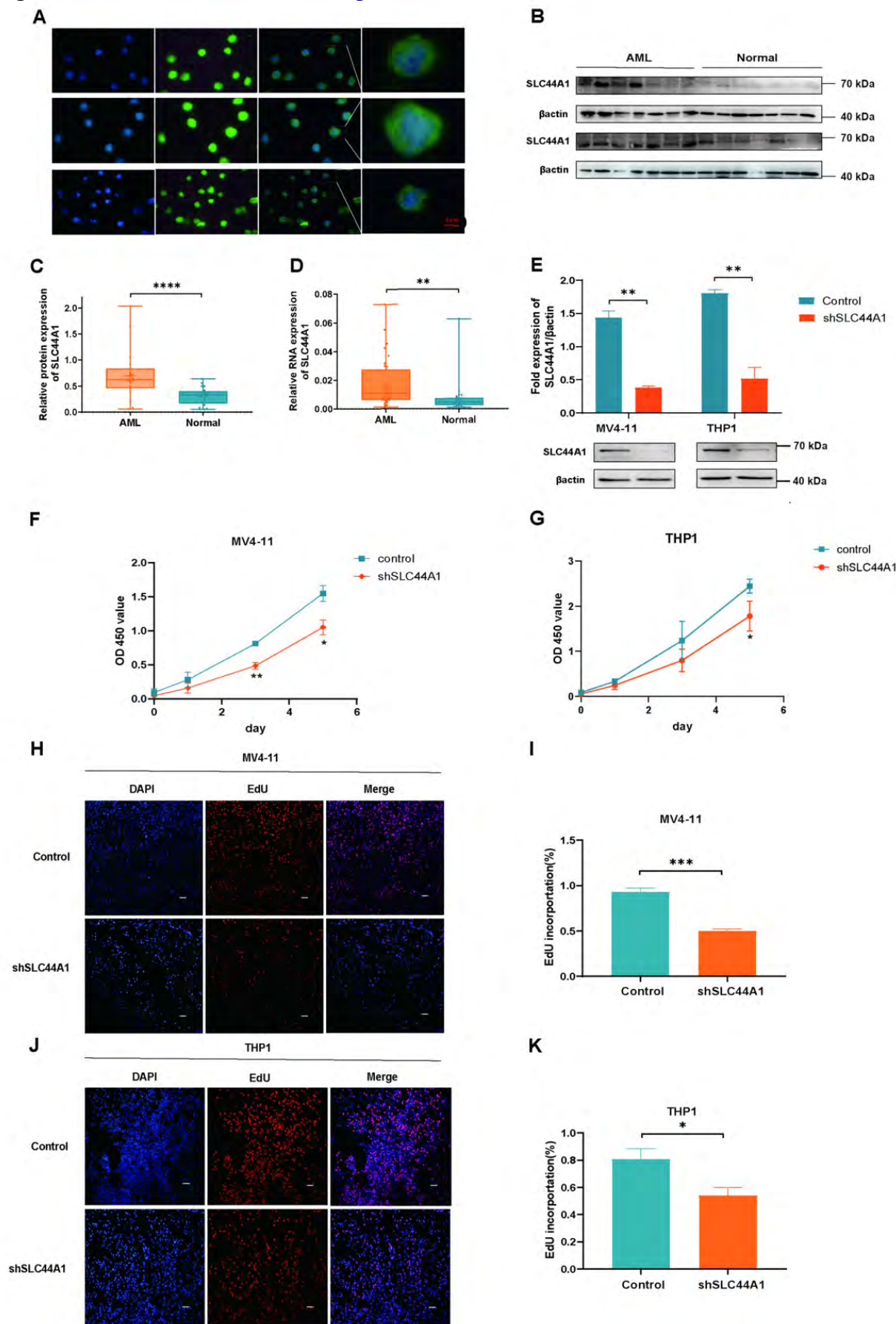


Fig. 2 [Download full resolution image](#)

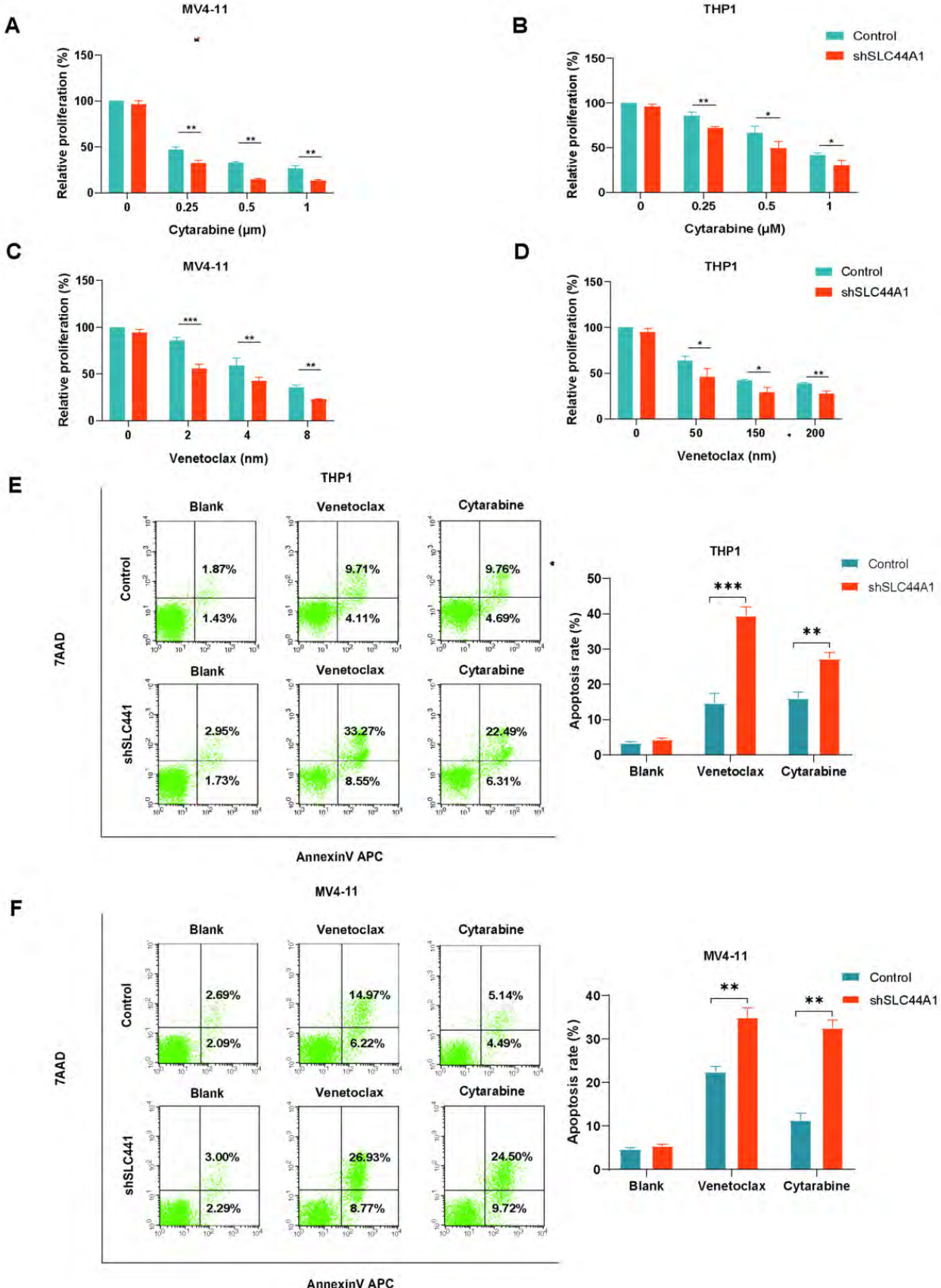


Fig. 3 [Download full resolution image](#)

